

# Wide-Field Fundus Autofluorescence Abnormalities and Visual Function in Patients With Cone and Cone-Rod Dystrophies

Maho Oishi, Akio Oishi, Ken Ogino, Yukiko Makiyama, Norimoto Gotoh, Masafumi Kurimoto, and Nagahisa Yoshimura

Department of Ophthalmology and Visual Sciences, Kyoto University Graduate School of Medicine, Kyoto, Japan

Correspondence: Akio Oishi, Department of Ophthalmology and Visual Sciences, Kyoto University Graduate School of Medicine, 54 Kawahara, Shogoin, Sakyo, Kyoto 606-8507, Japan; [aquio@kuhp.kyoto-u.ac.jp](mailto:aquio@kuhp.kyoto-u.ac.jp)

Submitted: January 8, 2014  
Accepted: April 4, 2014

Citation: Oishi M, Oishi A, Ogino K, et al. Wide-field fundus autofluorescence abnormalities and visual function in patients with cone and cone-rod dystrophies. *Invest Ophthalmol Vis Sci*. 2014;55:3572-3577. DOI: 10.1167/iov.14-13912

**PURPOSE.** To evaluate the clinical utility of wide-field fundus autofluorescence (FAF) in patients with cone dystrophy and cone-rod dystrophy.

**METHODS.** Sixteen patients with cone dystrophy (CD) and 41 patients with cone-rod dystrophy (CRD) were recruited at one institution. The right eye of each patient was included for analysis. We obtained wide-field FAF images using an ultra-widefield retinal imaging device and measured the area of abnormal FAF. The association between the area of abnormal FAF and the results of visual acuity measurements, kinetic perimetry, and electroretinography (ERG) were investigated.

**RESULTS.** The mean age of the participants was  $51.4 \pm 17.4$  years, and the mean logarithm of the minimum angle of resolution was  $1.00 \pm 0.57$ . The area of abnormal FAF correlated with the scotoma measured by the Goldman perimetry I/4e isopter ( $\rho = 0.79$ ,  $P < 0.001$ ). The area also correlated with amplitudes of the rod ERG ( $\rho = -0.63$ ,  $P < 0.001$ ), combined ERG a-wave ( $\rho = -0.72$ ,  $P < 0.001$ ), combined ERG b-wave ( $\rho = -0.66$ ,  $P < 0.001$ ), cone ERG ( $\rho = -0.44$ ,  $P = 0.001$ ), and flicker ERG ( $\rho = -0.47$ ,  $P < 0.001$ ).

**CONCLUSIONS.** The extent of abnormal FAF reflects the severity of functional impairment in patients with cone-dominant retinal dystrophies. Fundus autofluorescence measurements are useful for predicting retinal function in these patients.

**Keywords:** cone dystrophy, cone-rod dystrophy, fundus autofluorescence

Inherited retinal dystrophy is a major cause of blindness in developed countries.<sup>1</sup> The disease affects more than 2 million patients worldwide, and multiple causative genes have been identified.<sup>2</sup> Inherited retinal dystrophy can be categorized in four major groups: rod-dominant diseases, cone-dominant diseases, generalized retinal degenerations, and vitreoretinal disorders.<sup>2</sup> Cone dystrophy (CD) and cone-rod dystrophy (CRD) represent types of cone-dominant dystrophy.<sup>2</sup> Patients with panretinal cone-dominant degeneration are diagnosed with CD when rod function is preserved and diagnosed with CRD when rod function is impaired.

Rod functions are impaired relatively early in patients with CRD.<sup>3</sup> In addition, those who were originally diagnosed with CD can exhibit rod dysfunction once the condition has advanced.<sup>3,4</sup> The remaining rod photoreceptors and peripheral retinal function determine the extent of visual field loss, which is critical to a patient's quality of life.<sup>4</sup> Although electroretinography (ERG) is a standard technique for objectively evaluating the extent of remaining rod function, the examination is not easy to perform repeatedly in daily clinical practice.

Fundus autofluorescence (FAF) imaging is a noninvasive modality that allows the researcher to evaluate the status of photoreceptor cells and the retinal pigment epithelium. This technique can be used to visualize the distribution of lipofuscin and other fluorophores in these tissues; an increased FAF signal is thought to reflect the abnormal accumulation of fluorophores, whereas a decreased FAF signal seems to result from atrophy of

the RPE.<sup>5-7</sup> In addition, a recent study showed that disruption of the outer retina causes increased FAF.<sup>8</sup> All of these changes can be associated with retinal dysfunction. In fact, previous studies reported several characteristic FAF abnormalities in inherited retinal dystrophies, such as retinitis pigmentosa,<sup>9-15</sup> Stargardt disease,<sup>16-19</sup> CD, and CRD.<sup>19-21</sup> However, conventional FAF imaging approaches have focused largely on the central 30-55° of the fundus due to the angle of view possible with the devices used for autofluorescence imaging. There is little available information about peripheral FAF in CD or CRD.

The Optos (Optos PLC, Dunfermline, UK) is a novel wide-field imaging device that allows for a 200° view of the retina, rendering the retinal periphery easily accessible to photography and evaluation.<sup>22</sup> Several studies have reported the utility of Optos technology for the evaluation of FAF in chorioretinitis,<sup>23</sup> retinal detachment,<sup>24</sup> age-related macular degeneration,<sup>25</sup> and retinitis pigmentosa.<sup>13</sup> In this study, we examined wide-field FAF images of patients with CD and CRD and compared the associated findings with other clinical parameters including visual acuity as well as the results of Goldmann perimetry (GP) and ERG.

## METHODS

We examined consecutive patients with CD or CRD who visited the Department of Ophthalmology and Visual Sciences, Kyoto

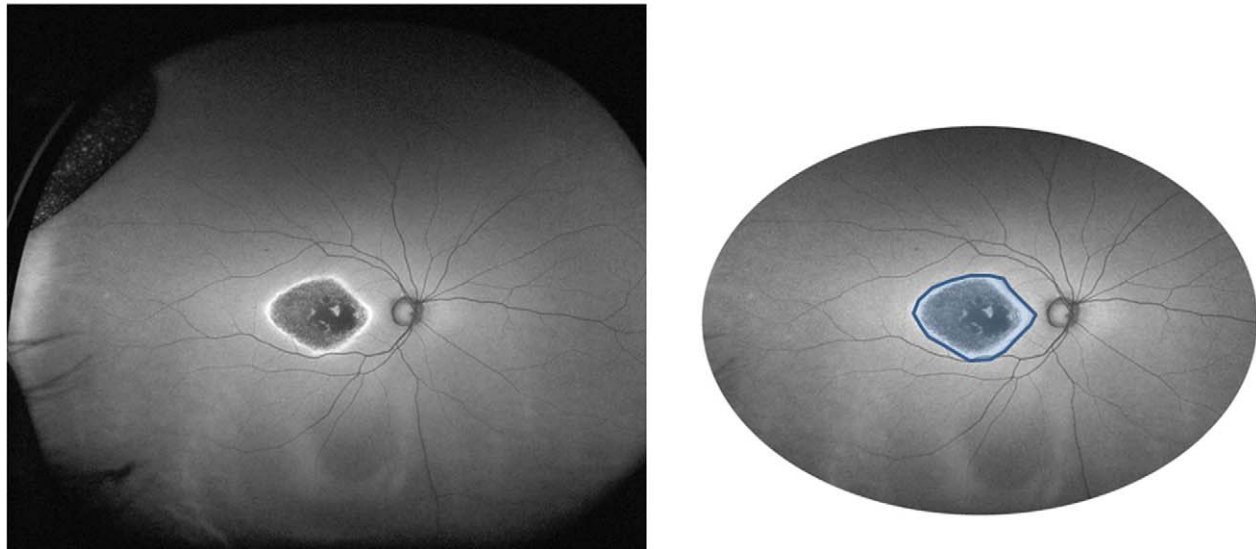


**FIGURE 1.** A wide-field FAF image of an eye with cone-rod dystrophy (*left*) and the measurement method employed in the present study. The measurement was done within the  $3000 \times 2100$ -pixel elliptical area. The area containing abnormal hyper- and hypo-FAF was traced, and the percentage within the elliptical area was calculated (*right*).

University Graduate School of Medicine, Kyoto, Japan during the period from March 2012 through November 2013. The protocol of the study adhered to the tenets of the Declaration of Helsinki. Approval was obtained from the Institutional Review Board (IRB)/Ethics Committee of the Kyoto University Graduate School of Medicine. The aim of the study and the measurement procedures were explained to the study participants; written informed consent was obtained from each participant.

Each patient's diagnosis was agreed upon by two retinal specialists (AO, MO). The diagnosis of CD was based on a progressive decline in visual acuity, the presence of a central scotoma, and reduced cone responses on full-field ERG, with normal rod responses. Full-field ERG was recorded according to the protocol recommended by the International Society for Clinical Electrophysiology of Vision (ISCEV) 2008.<sup>26</sup> Cone-rod dystrophy was diagnosed when the patient exhibited a progressive decline in visual acuity, a central scotoma, and reduced cone and rod responses on full-field ERG, with cone function equally or more severely reduced than rod function. Atrophic changes to the macular were confirmed in each patient using ophthalmoscopy and OCT images. When the two graders disagreed with regard to the diagnosis, another retinal specialist (KO) arbitrated. We excluded patients with Stargardt disease, central areolar choroidal dystrophy, pattern dystrophy, vitelliform macular dystrophy, age-related macular degeneration, rod-cone dystrophy, cystoid macular edema, syndromic disorders, and systemic disease such as a malignant tumor or hematological malignancy. Patients with a media opacity that impaired image quality were also excluded. The right eye of each patient was chosen for analysis.

### Clinical Assessment

We determined each patient's inheritance trait based on his or her family history. Best-corrected visual acuity was obtained from each patient using Landolt C charts. These values were then converted to the logMAR equivalent. All patients underwent dilated slit-lamp biomicroscopy, fundus examinations, and OCT imaging, which was performed using a spectral domain-OCT device (Spectralis; Heidelberg Engineering, Germany). As stated above, full-field ERG recording was performed

according to the recommendations of the ISCEV 2008.<sup>26</sup> The protocol includes the following settings: dark-adapted 0.01 ERG (rod response); dark-adapted 3.0 ERG (combined rod-cone response); light-adapted 3.0 ERG (cone response); light-adapted 3.0 flicker (30-Hz flicker). The amplitude of each component was used for subsequent analyses.

### Visual Field

Visual field testing was performed using a Goldmann perimeter (Haag Streit, Bern, Germany). The results were scanned and analyzed with ImageJ software (<http://imagej.nih.gov/ij/>; provided in the public domain by the National Institutes of Health, Bethesda, MD, USA). The magnification scale was calibrated first using the radius of the central  $90^\circ$  as is presented on standard recording paper. Under this system of calibration, a length of 632 pixels was equivalent to 10.8 cm on the visual field recording paper. The scotoma area, as defined by the  $1/4$  white test light, was traced and measured with the software. We included the blind spot of Mariotte when it was included within the extended scotomal area. The results were given in square centimeter units.

### Wide-Field Fundus Autofluorescence

Wide-field fundus photographs and FAF images were obtained with a ultra-widefield retinal imaging system. This instrument uses green light at 532 nm for excitation and captures the emitted signal with a detector for light from 570–780 nm. Although the retinal imaging system (Optos PLC) can acquire images from a nonmydriatic eye, we routinely dilated the pupils for concurrent OCT scans and ophthalmoscopic examinations.

We measured the area of abnormal FAF with ImageJ software (<http://imagej.nih.gov/ij/>; provided in the public domain by the National Institutes of Health, Bethesda, MD, USA). Any area of hypoautofluorescence or hyperautofluorescence was considered as abnormal FAF. To reduce the influence of eyelashes or eyelid shadow, we first excluded the most peripheral part of the image and cropped an elliptical area of  $3000 \times 2100$  pixels from the original  $3900 \times 3072$ -pixel image for analysis (Fig. 1). Two of the authors (MO, AO), who were blinded to the patients' clinical characteristics, measured each image individually; the

**TABLE.** The Results of Clinical Assessments and the Correlation With Area of Abnormal FAF

| Characteristics                        | Mean $\pm$ SD    | $\rho$ | P Value |
|--|------------------|--------|---------|
| Age, y                                 | 51.4 $\pm$ 17.4  | -0.09  | 0.51    |
| LogMAR VA                              | 1.00 $\pm$ 0.57  | 0.23   | 0.08    |
| GP I/4e scotoma size, cm <sup>2*</sup> | 18.8 $\pm$ 16.9  | 0.79   | <0.001  |
| Full-field ERG, $\mu$ V                |                  |        |         |
| Dark-adapted 0.01                      | 44.0 $\pm$ 35.0  | -0.63  | <0.001  |
| Dark-adapted 3.0 A wave                | 88.1 $\pm$ 59.0  | -0.72  | <0.001  |
| Dark-adapted 3.0 B wave                | 127.2 $\pm$ 83.2 | -0.66  | <0.001  |
| Light-adapted 3.0 B wave               | 43.1 $\pm$ 34.7  | -0.44  | <0.001  |
| Light-adapted 3.0 flicker, 30 Hz       | 37.5 $\pm$ 30.0  | -0.47  | <0.001  |

$\rho$ , correlation coefficient with the area of abnormal FAF; logMAR VA, logarithm of minimum angle of resolution visual acuity.

\* Eight patients who were unable to detect the I/4e white test light were excluded.

mean value was used for analysis. The results obtained as pixel values were converted into a percentage of the elliptical area analyzed (abnormal FAF area/analyzed area).

### Statistical Analyses

Statistical analyses were performed using statistical software (SPSS version 21.0; SPSS Science, Chicago, IL, USA). The results of descriptive analyses are reported as the mean  $\pm$  standard deviation. Associations between clinical characteristics and the area of abnormal FAF were assessed with Spearman's rank correlation test. A *P* value of <0.05 was considered statistically significant.

## RESULTS

### Clinical Characteristics

We enrolled a total of 63 patients. Wide-field FAF was successfully performed in all cases. None of the patients

complained of a deterioration in visual function or discomfort after the examination. After excluding two patients with poor-quality images and four patients who were found to share consanguinity with other participants, we evaluated 57 eyes of 57 patients (32 men and 25 women). The mean age was 51.4  $\pm$  17.4 years (range, 12–82 years), and the mean logMAR score was 1.00  $\pm$  0.57 units (range, 0–2 units). The study included 16 CD patients and 41 CRD patients. The inheritance pattern was autosomal dominant in 12 patients, autosomal recessive in 11 patients, X-linked in one patient, and sporadic in 33 patients. Thirty-two participants had previously submitted to causative mutation screening. The results showed *ABCA4* mutations in six patients (four CD patients and two CRD patients), *GUCY2D* mutations in two CD patients, and a *CRX* mutation in one CRD patient. There were no significant correlations between the area of abnormal FAF and age or logMAR score.

### Correlation Between the Results of Visual Field and FAF Examinations

The scotoma size measurements obtained by Goldmann perimetry are presented in the Table. Eight patients could not recognize the I/4e white test light anywhere in the visual field. All of these were the patients with abnormal FAF throughout the fundus, who were excluded from the corresponding analysis. Even after excluding these patients, scotoma size correlated well with the area of abnormal FAF (Figs. 2, 3).

### Correlation Between the Results of Electroretinography and FAF Examinations

The results of the full-field ERG examinations are presented as mean  $\pm$  standard deviation in the Table. The area of abnormal FAF correlated well with ERG results under all conditions. The larger the area of abnormal FAF, the smaller the amplitude of ERG recordings (Fig. 3). The correlation was relatively strong

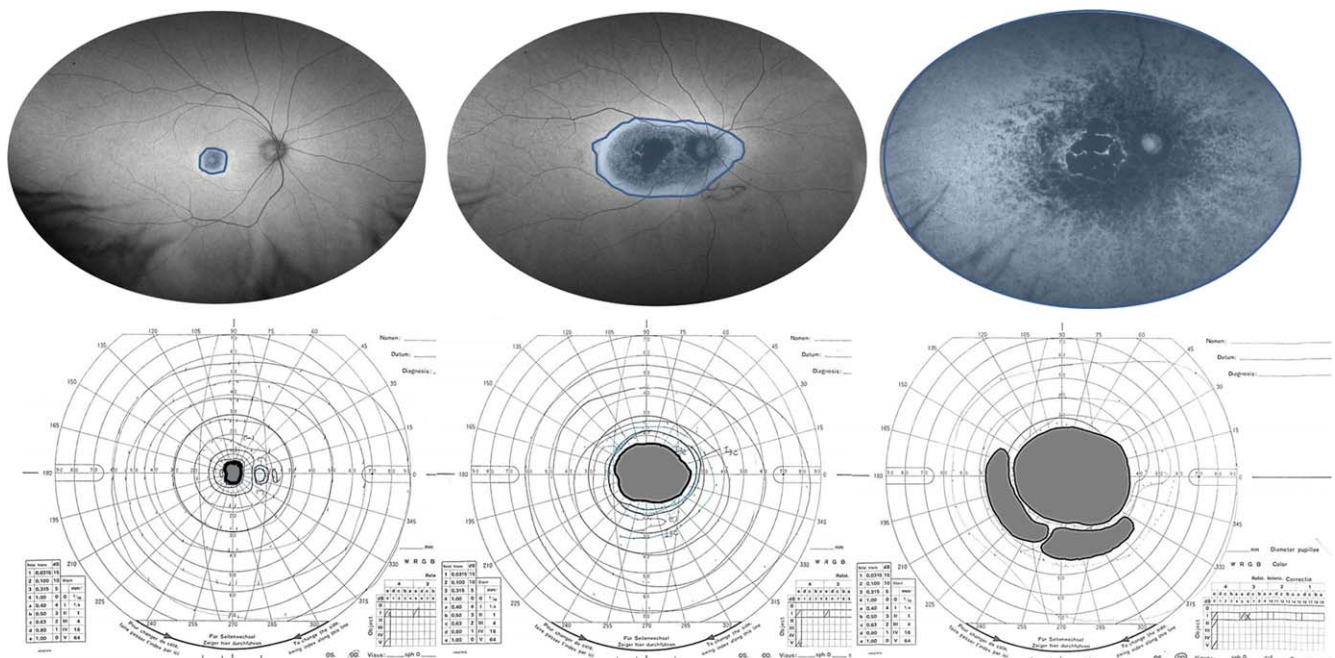


**FIGURE 2.** Representative images of wide-field fundus autofluorescence and Goldmann perimetry of eyes with cone or cone-rod dystrophy. Note that cases with larger areas of abnormal FAF showed larger scotoma areas defined by the I/4e white test light (area segmented in gray, lower row).

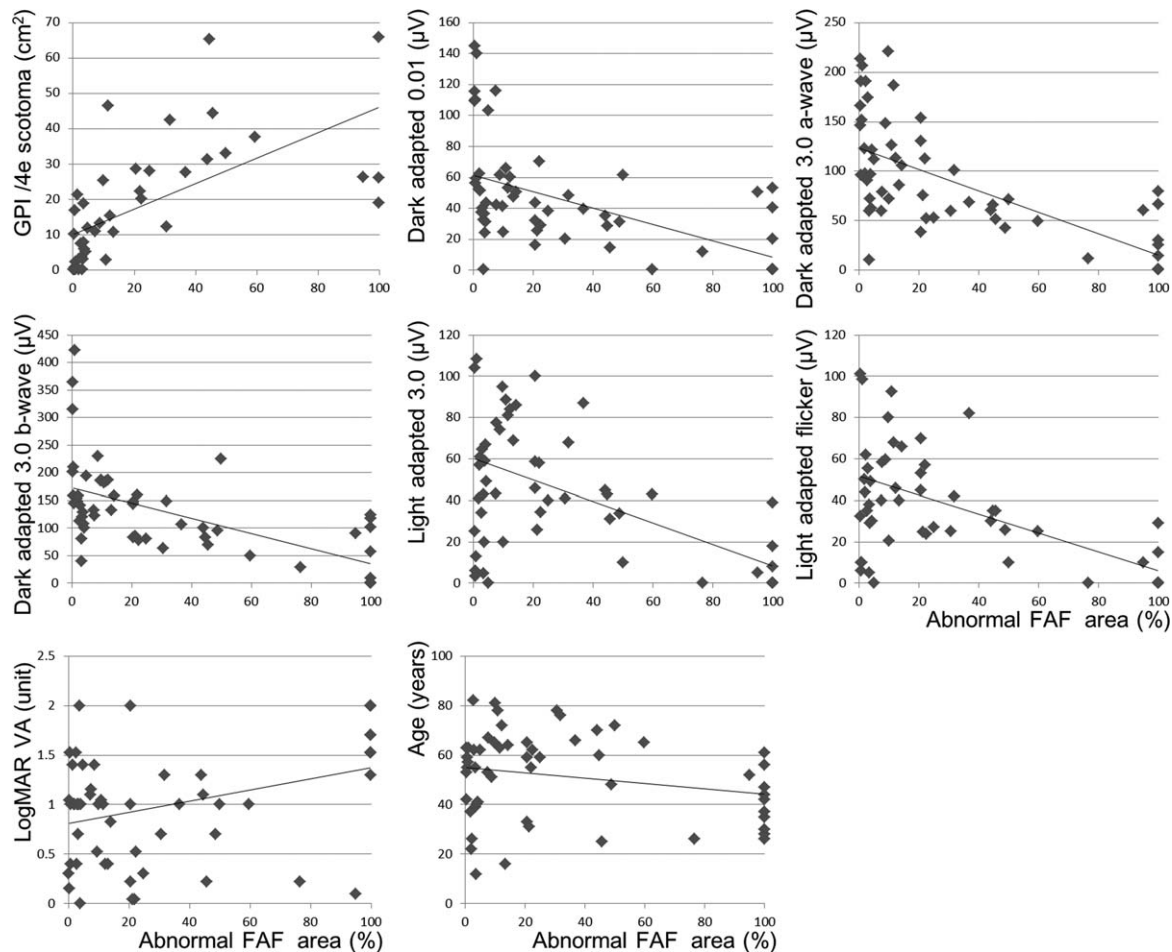


**FIGURE 3.** Scatter plots showing the relationship between the area of abnormal FAF and clinical characteristics. The area of abnormal FAF correlated well with visual function results on Goldman perimetry or ERG. The area of abnormal FAF showed no correlation with visual acuity or age.

in rod as well as combined responses and moderate for cone and flicker responses.

## DISCUSSION

In the present study, we used wide-field FAF to evaluate patients with CD and CRD. The results showed that the extent of abnormal FAF correlates with the visual field and the results of ERG. This result demonstrates that wide-field FAF is clinically useful for predicting visual function in patients with CD and CRD.

The area of abnormal FAF was associated with scotoma size as measured with GP. In addition, the location and size of the scotoma seemed to correspond to the area of abnormal FAF as shown in Figure 2. The association between abnormal FAF and visual field defects was consistent with our previous report on retinitis pigmentosa.<sup>13</sup> The present findings confirm the relationship between abnormal FAF and visual field defects in patients with CD or CRD as well as rod-dominant retinal dystrophy.

The association between the area of abnormal FAF and retinal function was also confirmed by the results of full-field ERG. The amplitude of the rod, cone, or combined responses decreased as the area of abnormal FAF increased, which would be expected considering the close correlation between visual field defects and changes in ERG amplitude.<sup>27</sup> We consider that

the use of wide-field FAF rather than conventional macular FAF is a reason for the strong correlation. Wide-field FAF can evaluate the peripheral retina; thus, the measurement correlated well with the results of GP or full-field ERG, which reflects function throughout the retina.

The association between cone function and the area of abnormal FAF was weaker than that of rod function and abnormal FAF area. This evidence suggests that FAF mainly reflects the function of rod photoreceptors. For example, the distribution of FAF roughly matches the distribution of rod photoreceptors.<sup>28</sup> In addition, the number of foveal cone-derived phagosomes in the RPE was one-third that of extrafoveal rod-derived phagosomes.<sup>29</sup> Larger areas of abnormal FAF represent more advanced stages or more severe phenotypes of the disease as manifest in rod function. Therefore, the association between larger areas of abnormal FAF and more pronounced cone dysfunction might reflect disease severity rather than cone cell loss itself.

There was no significant association between visual acuity and the area of abnormal FAF, as was expected from the nature of the examination. While the wide-field imaging device (Optos PLC) obtains a wide-field view of the retina, visual acuity only reflects foveal function. More specific examination tools such as static perimetry, microperimetry, contrast sensitivity measurement, and focal macular ERG would be more suitable for evaluating foveal function. Appropriate examinations should be employed to evaluate the area or the function of interest.

Previous studies focused on a ring of hyper-FAF around the degenerated retina. The finding was reported for patients with retinitis pigmentosa,<sup>14,15</sup> autoimmune retinopathy,<sup>30</sup> and age-related macular degeneration, respectively.<sup>31,32</sup> The increase in FAF adjacent to the atrophic area is considered to represent the presence of melanolipofuscin or changes in the metabolic activity of RPE cells.<sup>7</sup> This change sometimes precedes a visible change in appearance or retinal function<sup>7</sup> and is attracting attention. For example, in patients with retinitis pigmentosa, the size of the ring is associated with visual function,<sup>9,10</sup> and the radius of the ring constricts as the disease progresses.<sup>14</sup> As shown in the figures, the hyper-FAF ring was generally confirmed in cases whose decreased FAF area was confined to the area surrounding arcade vessels. Patients with decreased FAF that extends to the periphery will rarely, if ever, exhibit such a ring. One reason for the absence of the ring in advanced cases would be the distribution of lipofuscin: highest at approximately 10° from the fovea then decreasing toward the periphery.<sup>33</sup> The decreased background FAF may make it difficult to identify hyperautofluorescence in the periphery. Although we compared the clinical characteristics of patients with and without the ring, there was no significant difference. To evaluate the significance of the ring in CD and CRD, a longitudinal study is required.

Notably, this study included patients with CD and CRD. Although these diseases are differentiated clinically, they share major characteristics and there can be overlap between them.<sup>34</sup> For example, patients with CD can manifest rod dysfunction in the advanced stage of disease.<sup>3,4</sup> There is also overlap among the genes believed to cause these diseases.<sup>2,3,35</sup> Therefore, physicians must assess visual function in each patient without presumptions based upon the initial clinical diagnosis. The present results showed that the FAF pattern can roughly indicate the associated degree of retinal function regardless of a patient's clinical diagnosis. Accordingly, we might be able to evaluate patients with cone-dominant dystrophy to elaborate a spectrum of disease severity. Considering the difficulty in differentiating various manifestations of cone-dominant dystrophy, especially in advanced stages of disease, such an examination would facilitate patient treatment.

The present study has several limitations, including its cross-sectional study design and the relatively small number of patients, which was determined by the disease's prevalence. In addition, we had to exclude eight patients who did not respond to the 1/4e isopter from the analysis. If these patients had been included, the difference between type 3 and type 1 or 2 would have been larger. Submitting each patient to mutation identification would have furthered our understanding.

Finally, we demonstrated the close correlation of wide-field FAF findings and visual function in CD and CRD. This type of noninvasive examination can be a practical indicator of the patient's visual field and retinal responses to light. Longitudinal studies will be necessary to further characterize the related decline in visual function. The findings would serve as a clinical guide when diagnosing, evaluating, or following patients with CD or CRD.

### Acknowledgments

Supported in part by the Japan Ministry of Health, Labor and Welfare (No. 12103069).

Disclosure: **M. Oishi**, None; **A. Oishi**, None; **K. Ogino**, None; **Y. Makiyama**, None; **N. Gotoh**, None; **M. Kurimoto**, None; **N. Yoshimura**, Canon (F), Topcon (F), Nidek (F, C)

### References

- Hartong DT, Berson EL, Dryja TP. Retinitis pigmentosa. *Lancet*. 2006;368:1795-1809.
- Berger W, Kloeckener-Gruissem B, Neidhardt J. The molecular basis of human retinal and vitreoretinal diseases. *Prog Retin Eye Res*. 2010;29:335-375.
- Traboulsi EI. Cone dysfunction syndromes, cone dystrophies, and cone-rod degenerations. In: Traboulsi EI, ed. *Genetic Diseases of the Eye*. New York: Oxford University Press; 2012: 410-420.
- Thiadens AA, Phan TM, Zekveld-Vroon RC, et al. Clinical course, genetic etiology, and visual outcome in cone and cone-rod dystrophy. *Ophthalmology*. 2012;119:819-826.
- Delori FC, Dorey CK, Staurenghi G, Arend O, Goger DG, Weiter JJ. In vivo fluorescence of the ocular fundus exhibits retinal pigment epithelium lipofuscin characteristics. *Invest Ophthalmol Vis Sci*. 1995;36:718-729.
- Holz FG, Fleckenstein M, Schmitz-Valckenberg S, Bird AC. Evaluation of fundus autofluorescence images. In: Holz FG, Schmitz-Valckenberg S, Spaide RF, Bird AC, eds. *Atlas of Fundus Autofluorescence Imaging*. Berlin: Springer-Verlag; 2007:71-76.
- Schmitz-Valckenberg S, Holz FG, Bird AC, Spaide RF. Fundus autofluorescence imaging: review and perspectives. *Retina*. 2008;28:385-409.
- Freund KB, Mrejen S, Jung J, Yannuzzi LA, Boon CJ. Increased fundus autofluorescence related to outer retinal disruption. *JAMA Ophthalmol*. 2013;131:1645-1649.
- Robson AG, Egan CA, Luong VA, Bird AC, Holder GE, Fitzke FW. Comparison of fundus autofluorescence with photopic and scotopic fine-matrix mapping in patients with retinitis pigmentosa and normal visual acuity. *Invest Ophthalmol Vis Sci*. 2004;45:4119-4125.
- Robson AG, Saihan Z, Jenkins SA, et al. Functional characterisation and serial imaging of abnormal fundus autofluorescence in patients with retinitis pigmentosa and normal visual acuity. *Br J Ophthalmol*. 2006;90:472-479.
- Murakami T, Akimoto M, Ooto S, et al. Association between abnormal autofluorescence and photoreceptor disorganization in retinitis pigmentosa. *Am J Ophthalmol*. 2008;145:687-694.
- Fleckenstein M, Charbel Issa P, Fuchs HA, et al. Discrete arcs of increased fundus autofluorescence in retinal dystrophies and functional correlate on microperimetry. *Eye (Lond)*. 2009;23: 567-575.
- Oishi A, Ogino K, Makiyama Y, Nakagawa S, Kurimoto M, Yoshimura N. Wide-field fundus autofluorescence imaging of retinitis pigmentosa. *Ophthalmology*. 2013;120:1827-1834.
- Lima LH, Burke T, Greenstein VC, et al. Progressive constriction of the hyperautofluorescent ring in retinitis pigmentosa. *Am J Ophthalmol*. 2012;153:718-727. e711-712.
- Lima LH, Cella W, Greenstein VC, et al. Structural assessment of hyperautofluorescent ring in patients with retinitis pigmentosa. *Retina*. 2009;29:1025-1031.
- Lois N, Halfyard AS, Bird AC, Holder GE, Fitzke FW. Fundus autofluorescence in Stargardt macular dystrophy-fundus flavimaculatus. *Am J Ophthalmol*. 2004;138:55-63.
- Smith RT, Gomes NL, Barile G, Busuioc M, Lee N, Laine A. Lipofuscin and autofluorescence metrics in progressive STGD. *Invest Ophthalmol Vis Sci*. 2009;50:3907-3914.
- Cukras CA, Wong WT, Caruso R, Cunningham D, Zein W, Sieving PA. Centrifugal expansion of fundus autofluorescence patterns in Stargardt disease over time. *Arch Ophthalmol*. 2012;130:171-179.
- Kellner S, Kellner U, Weber BH, Fiebig B, Weinitz S, Ruether K. Lipofuscin- and melanin-related fundus autofluorescence in patients with ABCA4-associated retinal dystrophies. *Am J Ophthalmol*. 2009;147:895-902. 902 e891.
- von Ruckmann A, Fitzke FW, Bird AC. In vivo fundus autofluorescence in macular dystrophies. *Arch Ophthalmol*. 1997;115:609-615.

21. Robson AG, Michaelides M, Luong VA, et al. Functional correlates of fundus autofluorescence abnormalities in patients with RPGR or RIMS1 mutations causing cone or cone rod dystrophy. *Br J Ophthalmol*. 2008;92:95-102.
22. Manivannan A, Plskova J, Farrow A, McKay S, Sharp PF, Forrester JV. Ultra-wide-field fluorescein angiography of the ocular fundus. *Am J Ophthalmol*. 2005;140:525-527.
23. Seidensticker F, Neubauer AS, Wasfy T, et al. Wide-field fundus autofluorescence corresponds to visual fields in chorioretinitis patients. *Clin Ophthalmol*. 2011;5:1667-1671.
24. Witmer MT, Cho M, Favarone G, Chan RV, D'Amico DJ, Kiss S. Ultra-wide-field autofluorescence imaging in non-traumatic rhegmatogenous retinal detachment. *Eye (Lond)*. 2012;26:1209-1216.
25. Witmer MT, Kozbial A, Daniel S, Kiss S. Peripheral autofluorescence findings in age-related macular degeneration. *Acta Ophthalmol*. 2012;90:e428-433.
26. Marmor MF, Fulton AB, Holder GE, Miyake Y, Brigell M, Bach M. ISCEV Standard for full-field clinical electroretinography (2008 update). *Doc Ophthalmol*. 2009;118:69-77.
27. Zahid S, Jayasundera T, Rhoades W, et al. Clinical phenotypes and prognostic full-field electroretinographic findings in Stargardt disease. *Am J Ophthalmol*. 2013;155:465-473. e463.
28. Curcio CA, Sloan KR, Kalina RE, Hendrickson AE. Human photoreceptor topography. *J Comp Neurol*. 1990;292:497-523.
29. Anderson DH, Fisher SK, Erickson PA, Tabor GA. Rod and cone disc shedding in the rhesus monkey retina: a quantitative study. *Exp Eye Res*. 1980;30:559-574.
30. Lima LH, Greenberg JP, Greenstein VC, et al. Hyperautofluorescent ring in autoimmune retinopathy. *Retina*. 2012;32:1385-1394.
31. Bindewald A, Schmitz-Valckenberg S, Jorzik JJ, et al. Classification of abnormal fundus autofluorescence patterns in the junctional zone of geographic atrophy in patients with age related macular degeneration. *Br J Ophthalmol*. 2005;89:874-878.
32. Holz FG, Bindewald-Wittich A, Fleckenstein M, Dreyhaupt J, Scholl HP, Schmitz-Valckenberg S. Progression of geographic atrophy and impact of fundus autofluorescence patterns in age-related macular degeneration. *Am J Ophthalmol*. 2007;143:463-472.
33. Delori FC, Goger DG, Dorey CK. Age-related accumulation and spatial distribution of lipofuscin in RPE of normal subjects. *Invest Ophthalmol Vis Sci*. 2001;42:1855-1866.
34. van den Biesen PR, Deutman AF, Pinckers AJ. Evolution of benign concentric annular macular dystrophy. *Am J Ophthalmol*. 1985;100:73-78.
35. Garcia-Hoyos M, Auz-Alexandre CL, Almoguera B, et al. Mutation analysis at codon 838 of the Guanylate Cyclase 2D gene in Spanish families with autosomal dominant cone, cone-rod, and macular dystrophies. *Mol Vis*. 2011;17:1103-1109.